ELSEVIER

Applied Surface Science 104/105 (1996) 455-460

applied surface science

UV photoemission study of heteroepitaxial AlGaN films grown on 6H-SiC

M.C. Benjamin, M.D. Bremser, T.W. Weeks, Jr., S.W. King, R.F. Davis, R.J. Nemanich *

Department of Physics and Department of Materials Science and Engineering, North Carolina State University, Raleigh, NC 27695-8202, USA

Received 28 June 1995; accepted 10 October 1995

Abstract

This study presents results of UV photoemission measurements of the surface and interface properties of heteroepitaxial AlGaN on 6H-SiC. Previous results have demonstrated a negative electron affinity of AlN on 6H-SiC. In this study $Al_xGa_{1-x}N$ alloy films were grown by organometallic vapor phase epitaxy (OMVPE) and doped with silicon. The analytical techniques included UPS, Auger electron spectroscopy, and LEED. All analysis took place in an integrated UHV transfer system which included the analysis techniques, a surface processing chamber and a gas source MBE. The OMVPE alloy samples were transported in air to the surface characterization system while the AlN and GaN investigations were prepared in situ. The surface electronic states were characterized by surface normal UV photoemission to determine whether the electron affinity was positive or negative. Two aspects of the photoemission distinguish a surface that exhibits a NEA: (1) the spectrum exhibits a sharp peak in the low kinetic energy region, and (2) the width of the spectrum is $h\nu - E_g$. The in situ prepared AlN samples exhibited the characteristics of a NEA while the GaN and $Al_{0.13}Ga_{0.87}N$ samples did not. The $Al_{0.55}Ga_{0.45}N$ sample shows a low positive electron affinity. Annealing of the sample to > 400°C resulted in the disappearance of the sharp emission features, and this effect was related to contaminant effects on the surface. The results suggest the potential of nitride based cold cathode electron emitters.

1. Introduction

There is increasing interest in electronic devices composed of III-nitride materials for opto-electronic applications in the blue and UV region [1]. An alternative application of these semiconductors is in electron emission devices. Recent studies have demonstrated that diamond surfaces can exhibit a negative electron affinity (NEA). NEA surfaces may prove to be critical elements for cold cathode devices, vacuum microelectronics, and photodetectors [2,3]. In addition to diamond, thin films of AlN grown on 6H-SiC have been shown to exhibit a negative electron affinity (NEA) [4,5]. The AlN NEA surfaces were obtained from air exposed surfaces, and do not appear to be readily poisoned. In contrast to diamond, AlGaN materials exhibit the wurtzite crystal structure. One of the most significant limitations in the application of diamond is that reliable n-type doping has not been achieved. In contrast, n-type doping has been obtained for GaN and some

---

* Corresponding author. Tel.: +1-919-5153225; fax: +1-919-5157331; e-mail: robert_nemanich@ncsu.edu.

PII S0169-4332(96)00186-9

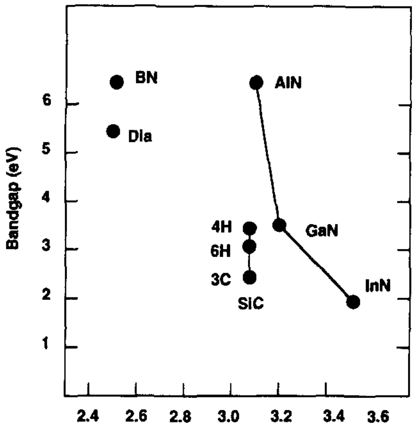

Fig. 1. The bandgap versus hexagonal lattice constant (a) for a variety of wide bandgap semiconductors. The lattice constant for the cubic materials has been determined from the (111) plane.

AlGaN alloys. This study explores further the electron affinity of epitaxial AlGaN films on 6H-SiC.

The wurtzite AlN and GaN form a continuous solid solution of $Al_xGa_{1-x}N$ for $0 \leq x \leq 1$ with bandgaps that range from 3.4 eV (GaN) to 6.2 eV (AlN). Fig. 1 displays the bandgap of several materials as a function of the equivalent hexagonal lattice constant. The alloys are also miscible with In, hence the inclusion of InN could extend the range to 1.9 eV. The electron affinity of a semiconductor is related to the surface dipole and to the fundamental energy levels of the materials. Because the valence and conduction bands of the semiconductors have origin in the sp^3 bonding and antibonding levels, it may be suggested that the larger bandgap materials will exhibit a smaller or negative electron affinity. In comparison with diamond, it might be assumed that AlGaN alloys with a bandgap greater that 5.4 eV could exhibit a NEA. In this paper we report studies of AlGaN with x values of 0.55 and 0.13 as well as preliminary studies of GaN.

The AlGaN and GaN films used in this study were grown on vicinal 6H-SiC substrates. The n-type SiC substrates used have a small lattice mismatch with AlN (3.08 Å versus 3.11 Å) and GaN (a = 3.19 Å). The small lattice mismatch enables heteroepitaxial growth of the wurtzite (2H) structure. Furthermore, the fact that the substrates are conducting avoids charging problems associated with photoemission from large bandgap and insulating materials.

The electron affinity of a semiconductor or the presence of a NEA can be determined by ultraviolet photoemission spectroscopy (UPS) [6–8]. The experiments described here involve directing 21.2 eV light (the He I resonance line) to the surface of the sample and detecting the spectrum of the emitted photo excited electrons as a function of electron kinetic energy. Typically, UPS is used to obtain a profile of the valence band (VB) electronic states. As such, most studies of UPS of semiconductors present data of the most energetic electrons emitted from the surface. Electrons scattered to lower energy and secondary electrons will be displayed in the spectrum at lower kinetic energies. In addition, for a semiconductor which exhibits a NEA surface, a distinctive peak may be observed at the low kinetic energy (highest binding energy) end of the photoemission spectra. Fig. 2 depicts a schematic representation of the photoemission spectra from a semiconductor with a negative or positive electron affinity. The low kinetic energy feature is due to secondary electrons which (quasi) thermalize to the conduction band minimum. Note that the solid line indicates a material with a positive electron affinity while the dashed line is a feature indicative of a NEA. In this paper we discuss samples with both positive and negative affinity surfaces.

The sharp features typical of a NEA have been observed from spectra of (111) and (100) diamond surfaces [6–10]. In the studies of diamond, a correlation was made between the presence of hydrogen and the NEA peak [9,10]. In addition, it was also

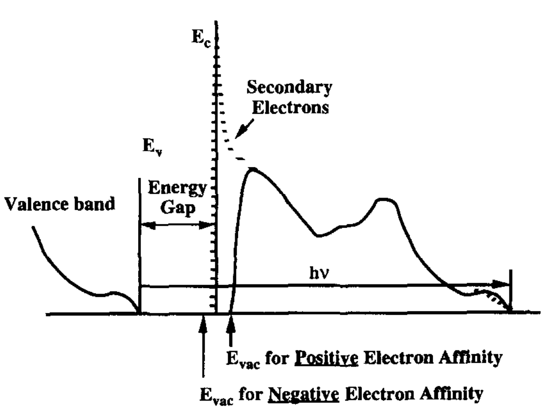

Fig. 2. A schematic of the difference in the photoemission spectra of a semiconductor with a positive or negative electron affinity.

shown that thin metal layers such as Ti or other moderate work function metals could induce a NEA on the diamond surface [10,11]. These measurements verify that the surface dipole can be influenced by surface processing and that the effects contribute to the observation of a NEA.

2. Experimental procedure

The 6H-SiC substrates used in this study were supplied by Cree Research, Inc. The samples were n-type with doping concentrations of 10^{16} to 10^{18} cm^{-3}. The AlGaN samples were grown by CVD in a remote location and transported in ambient to the analysis system. To avoid surface contamination AlN and GaN samples were also grown in the integrated UHV transfer system by gas source molecular beam epitaxy (GSMBE). This system includes the UPS system, LEED, Auger, hydrogen and argon plasma processing chamber, and XPS as well as the GSMBE. The system is described elsewhere [9,11]. Recently added is the capability of gas source MBE (GSMBE) to grow undoped AlN and GaN films.

The AlGaN thin films were grown on vicinal n-type, Si-face α(6H)-SiC(0001) substrates at 1100°C. Vicinal wafers were SiC(0001) 3°–4° off-axis toward the $\langle 11\bar{2}0 \rangle$. The as-received SiC wafers were cut into 7.1 mm squares. The SiC pieces were degreased, dipped into a 10% HF solution for 10 min to remove the thermally grown oxide layer, and blown dry with N_2 before being loaded onto the SiC-coated graphite susceptor. The reactor was evacuated to less than 3×10^{-5} Torr prior to initiating growth. The continuously rotating susceptor was rf inductively heated to the AlGaN deposition temperature of 1100°C in 3 SLM of flowing H_2 diluent. Hydrogen was also used as the carrier gas for the various metalorganic precursors. Once this growth temperature was reached and stabilized, AlGaN deposition was started by flowing triethylaluminum (TEA), triethylgallium (TEG) and ammonia (NH_3) into the reactor at 23.6 μmol/min, 10.5 μmol/min and 1.5 SLM, respectively. The approximate solid solution alloy concentration using these growth parameters was estimated to be $Al_{0.55}Ga_{0.45}N$ from cathodoluminescence measurements. The AlGaN films were doped with Si from a SiH_4 source (8.2 ppm in N_2 balance) at flow rates between 2.89 and 5 nmol/min to minimize charging problems. The system pressure during AlGaN growth was 45 Torr. The AlGaN layer was grown for 90 min resulting in an approximate thickness of 1.5 μm. AlGaN samples were transported in air to the analysis system. Film concentrations were determined from the bandgap values of cathodoluminescence. Auger electron spectroscopy was also used to characterize the surface.

The GaN growth took place in a GSMBE. The cleaning procedure is similar to the above described process but differs in that once in vacuum the substrate is annealed in a silane flux [12]. The GaN samples were not intentionally doped, but since very thin films were employed, charging problems were avoided.

The UPS measurements were excited with 21.21 eV radiation (He I resonance line), and emitted electrons are collected with a hemispherical energy analyzer. The base pressure of the UPS system is 2×10^{-10} Torr, and operating conditions involve pressures up to 1×10^{-9} Torr, but the higher pressure is due to the helium inflow and does not contaminate the sample. The 50 mm mean radius hemispherical electron analyzer was operated at a 0.15 eV energy resolution and a 2° angular resolution. The analyzer (VSW HA50) is mounted on a double goniometer and can be tilted with respect to the sample in two independent directions. The samples were fastened with tantalum wire to a molybdenum sample holder. The sample holder is biased by up to 3 V to allow low energy electrons to overcome the work function of the analyzer. The Fermi level of the system (sample and analyzer) is determined by UPS measurement of the sample holder with no sample bias (i.e., grounded). The sample holder can be heated to 1150°C, and the temperature is measured by a thermocouple.

3. Results and discussion

The UV photoemission spectra of all four samples studied here are shown in Fig. 3. The AlN and GaN films were prepared by gas source MBE and transferred under UHV to the photoemission system. The two alloy samples were prepared by CVD and suffered ambient exposure. Samples were biased with

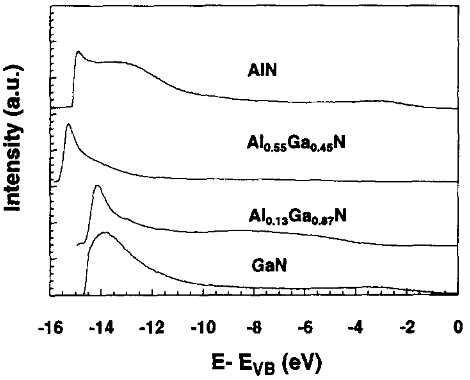

Fig. 3. The UV photoemission spectra of $Al_xGa_{1-x}N$ for $x = 0$, 0.13, 0.55, 1.0. Spectra were aligned at the valence band maximum.

2–3 V to overcome the work function of the analyzer, and all spectra were shifted to be aligned at the valence band maximum. The spectra were scaled such that the strongest emission was the same for all curves.

The first aspect to be noted is that the spectra of the 55% aluminum alloy and AlN exhibit sharp strong features at the highest binding energy, which corresponds to the lowest kinetic energy. These features are possibly indicative of a negative electron affinity. As noted in the introduction, the feature is attributed to emission from electrons quasi-thermalized to the conduction band minimum. The emission from the $Al_{0.13}Ga_{0.87}N$ sample is significantly weaker, and the GaN emission does not show the sharp peak at all.

A second indication of the change in electron affinity with alloy concentration is the extension of the $Al_xGa_{1-x}N$ spectra to lower energy as x is decreased. A more precise description of the relation of the NEA is obtained from the spectral width. The spectral width is obtained from a linear extrapolation of the emission onset edge to zero intensity at both the low kinetic energy cutoff and at the high kinetic energy end (reflecting the valence band maximum). For a material with a positive electron affinity, Fig. 2 shows that $\chi = h\nu - E_g - W$, and for a material with a negative electron affinity Fig. 2 indicates that $0 = h\nu - E_g - W$, or rewriting, $h\nu = E_g + W$. This analysis indicates that the 55% aluminum sample does not have a negative affinity but rather a low positive affinity value, as discussed below. We note that the photoemission measurements cannot be used to determine the energy position of the electron affinity for the NEA case.

To determine the energy position of the valence band maximum, the spectral gain was increased, and the intensity was extrapolated to 0 emission. The spectra are aligned in Fig. 3 at the deduced valence band maximum. The spectral widths obtained from the $Al_xGa_{1-x}N$ samples were 14.5, 14.5, 15.5, and 15 eV for $x = 0$, 0.13, 0.55, and 1.0, respectively. In applying the relations noted above, the bandgaps of the bulk AlN and GaN must also be known. The literature values of the AlN and GaN bandgaps are 6.2 and 3.4 eV respectively. Assuming a linear extrapolation for the bandgap of the alloys, we deduce $x = 0.55$ for $E_g = 4.70$ eV and $x = 0.13$ for $E_g = 3.80$ eV. Using the relations described above, the AlN surface satisfies the relations for a NEA within ±0.2 eV, while the GaN, $Al_{0.55}Ga_{0.45}N$, and the $Al_{0.13}Ga_{0.87}N$ surfaces do not satisfy the relations for a NEA. We can, however, determine the value of the electron affinity of these materials and find that $\chi = 3.3$ eV, 2.9 eV, and 1.0 eV for $x = 0$, 0.13, and 0.55, respectively.

Another aspect that is evident from the photoemission spectra is the position of the surface Fermi level relative to the valence band maximum. It was found that E_F ranges from 2 to 3.5 eV above the valence band maximum for each sample. For the GaN and $Al_{0.13}Ga_{0.87}N$ surfaces, these values position E_F in the upper part of the gap while for the AlN and 55% Al samples, the values indicate that the surface Fermi level is pinned near midgap. The pinning at midgap may be an indication of increased impurity incorporation. In particular, the strong affinity of Al with oxygen often results in increased oxygen incorporation for these films.

To further explore the surface affinity, the effect of annealing in vacuum was explored for the $x = 0.55$ sample. The results are shown in Fig. 4. After annealing to 475°C and 580°C for 10 min the photoemission spectra showed a decrease in the relative intensity of the NEA related peak. Furthermore, the width of the spectra also decreases. As these temperatures are much less than the temperatures involved in growth, it is unlikely that a component present during growth is removed. It is possible that we introduced some type of contamination which affected the emission. We suggest hydrocarbon contaminants as a likely possibility. No LEED pattern was visible for the $Al_{0.55}Ga_{0.45}N$ sample, and the lack of a LEED pattern for the as-loaded samples is possibly related to carbon and oxygen on the surface (attributed to the transport in air). The annealing may result in more complete bonding of the surface adsorbed hydrocarbon layer which results in a change in the surface dipole. Another possibility is that the electron affinity has been affected by adsorbed molecules such as hydrogen. While previous results have shown that hydrogen can induce a negative electron affinity surface on diamond [7,10], the AlGaN surfaces have not been intentionally exposed to H. It is evident that further studies are necessary to characterize the surfaces more completely.

The deduced electron affinities versus alloy concentration are shown in Fig. 5. Again we note that the photoemission measurements cannot be used to determine the position of the vacuum level for a NEA surface so this point is indicated at $\chi = 0$ with an arrow to larger negative values. The results suggest that the electron affinity depends on the alloy concentration as originally suggested. Unfortunately, we do not have sufficient data at this time to more completely describe the effect. Additionally, we have made no effort to control the surface termination for these samples. For diamond, it was found that the observation of a NEA is critically dependent on the surface termination. Future studies will explore whether the electron affinity of AlGaN materials is also affected by different surface preparations.

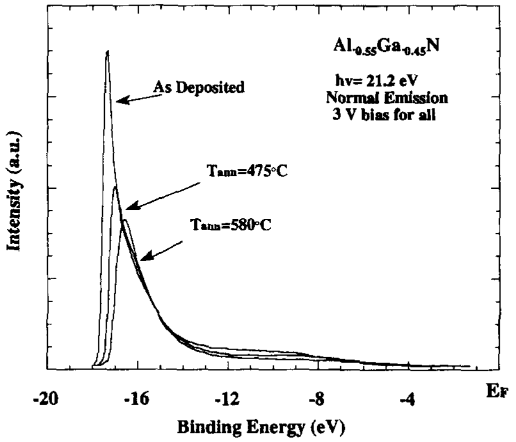

Fig. 4. The UV photoemission from $Al_{0.55}Ga_{0.45}N$ on 6H-SiC versus annealing temperature.

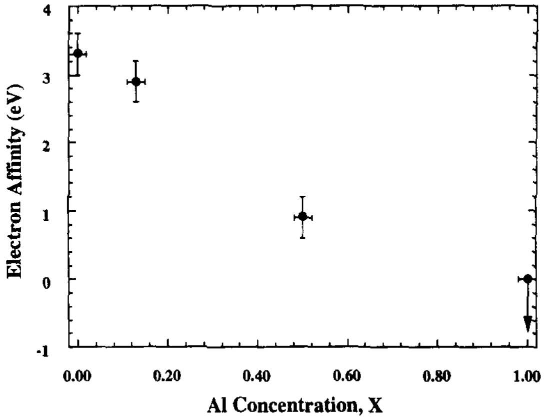

Fig. 5. Electron affinities of $Al_xGa_{1-x}N$ alloys versus Al concentration. The arrow indicates that the electron affinity is less than (or equal to) 0, but the value cannot be determined from the UV photoemission measurements.

4. Conclusions

In summary, we have observed features in the UPS spectra indicative of a NEA surface on AlN and a low positive electron affinity for $Al_{0.55}Ga_{0.45}N$. The AlN spectra exhibited both the sharp features at low kinetic energy that have been found to be characteristic of a NEA, and the width of the spectra was also consistent with the observed effect. The UPS spectra of AlGaN alloys did not show an NEA, but the measurements have been used to determined the electron affinity of GaN, $Al_{0.13}Ga_{0.87}N$, and $Al_{0.55}Ga_{0.45}N$ yielding values of 3.3, 2.9, and 1.0 eV, respectively.

The surface Fermi level was found to shift towards the middle of the band gap for the Al rich samples, and this may indicate an increase in oxygen impurities.

The NEA surfaces were robust showing the effect even after transfer through ambient. AlN samples grown in situ have shown NEA surfaces without the presence of oxygen. The positive affinity surfaces when annealed result in a change of the electron affinity. This effect was attributed to a change in the surface layer that affected the surface dipole.

Future work will involve examining samples to fill in the gaps in the solid solution of AlGaN alloys.

Furthermore, we will explore whether surface treatments can be employed on the AlGaN alloys to form stable NEA surfaces.

Acknowledgements

This work was supported in part by the Office of Naval Research through grants N0014-92-J-1477 and N0014-92-J-1604. The SiC substrates used were supplied by Cree Research. We thank Bill Perry for performing the cathodoluminescence measurements.

References

[1] S. Strite and H. Morkoç, J. Vac. Sci. Technol. B 10 (1992) 1237.
[2] J.H. Edgar, J. Mater. Res. 7 (1992) 235.
[3] M.D. Williams, M.D. Feuer, S.C. Shunk, N.J. Sauer and T.Y. Chang, J. Appl. Phys. 71 (1992) 3042.
[4] M.C. Benjamin, C. Wang, R.F. Davis and R.J. Nemanich, Appl. Phys. Lett. 64 (1994).
[5] M.C. Benjamin, C. Wang, R.S. Kern, R.F. Davis and R.J. Nemanich, Mater. Res. Soc. Symp. 339 (1994) 81.
[6] F.J. Himpsel, J.A. Knapp, J.A. van Vechten and D.E. Eastman, Phys. Rev. B 20 (1979) 624.
[7] B.B. Pate, Surf. Sci. 165 (1986) 83.
[8] B.B. Pate, M.H. Hecht, C. Binns, I. Lindau and W.E. Spicer, J. Vac. Sci. Technol. 21 (1982) 364.
[9] J. van der Weide and R.J. Nemanich, J. Vac. Sci. Technol. B 10 (1992) 1940.
[10] J. van der Weide and R.J. Nemanich, Appl. Phys. Lett. 62 (1993) 1878.
[11] J. van der Weide and R.J. Nemanich, Phys. Rev. B 15 (1994) 49, 13629.
[12] R. Kaplan, Surf. Sci. 215 (1989) 111.